Journal of Drug Delivery Science and Technology 96 (2024) 105699

Contents lists available at ScienceDirect

Journal of Drug Delivery Science and Technology

journal homepage: www.elsevier.com/locate/jddst

Microfluidic development of brain-derived neurotrophic factor loaded solid lipid nanoparticles: An *in vitro* evaluation in the post-traumatic brain injury neuroinflammation model

Federica Sommonte [a,1], Ilaria Arduino [a,1], Rosa Maria Iacobazzi [a], Luna Laera [b], Teresa Silvestri [a], Angela Assunta Lopedota [a], Alessandra Castegna [b], Nunzio Denora [a,*]

[a] Department of Pharmacy – Pharmaceutical Sciences, University of Bari "Aldo Moro", 70125, Bari, Italy
[b] Department of Biosciences, Biotechnologies, Environment, University of Bari, Bari, Italy

ARTICLE INFO

Keywords:
Solid lipid nanoparticles
Microfluidics
Brain-derived neurotrophic factor
Brain delivery
Traumatic brain injury
Neuroinflammation

ABSTRACT

Microfluidic-based nanoscale drug delivery systems have risen to prominence in the field of precision nanomedicine in recent years. This intriguing innovation could provide unique therapeutic prospects in the treatment of serious disorders as traumatic brain injury, a potentially fatal condition that is widespread during childhood. According to current scientific study, neurotrophins are vital for the healing of injured brain parenchyma, and the brain-derived neurotrophic factor (BDNF) in particular may have significant regenerative effects. To address BDNF-related pharmacokinetic constraints, microfluidic-assisted manufacturing of BDNF-loaded solid lipid nanoparticles (BDNF-SLNs) was carried out, and following evaluation, the formulation demonstrated optimum characteristics in terms of size (190.3 ± 10.1 nm), PDI (0.180 ± 0.023), and ζ-potential (– 39.2 ± 1.30 mV). Short-term stability studies and the haemolysis assay verified the formulation's biocompatibility, while an *in vitro* permeability analysis revealed an increase in the Papp of the encapsulated BDNF ($1.27x10^{-5}$ cm/s) as compared to plain BDNF ($9.31x10^{-6}$ cm/s). The *in vitro* mimicked neuroinflammatory model demonstrated an enhanced decrease in nitrite production and *Nos* mRNA levels using BDNF-SLNs compared to plain BDNF as a control, validating the proficiency of the microfluidic-based drug delivery systems as pioneering and valuable approaches for the brain delivery of biologicals.

1. Introduction

The central nervous system (CNS) constitutes the control system of the human body since it is skilled to manage any kind of incoming stimulation while keeping the fragile brain microenvironment strictly controlled. In this context, the blood-brain barrier (BBB) plays a pivotal role, representing a dynamic entity that serves as physical barrier, preventing non-specific stimulation and controlling the molecular traffic in and out of the brain tissue [1].

Among the plethora of CNS-related illnesses, the traumatic brain injury (TBI) is one of the most prominent. TBI is a comprehensive definition that refers to a multitude of impairments triggered by a traumatic event impacting the brain, and it appears to be a relevant public health concern since it has been identified as the main cause of long-term disability and/or death in children [2]. This pathological condition evolves in a biphasic manner. In the first place, the trauma (open or closed head) initially results in damage symptoms (e.g., edema), which then leads to a dysregulation of tight junctions and extracellular matrix, increasing BBB paracellular permeability and altering the activity and/or expression of physiological transporters [3,4]. Subsequently, the injury causes oxidative stress by boosting the synthesis of pro-inflammatory mediators turning into an extensive neuroinflammatory process [5,6]. Despite being widely recognized as a disruptive secondary phase, neuroinflammation presents a therapeutic opportunity to halt more tissue damage and function loss. In fact, the breakdown of the BBB allows for passively directing non-invasive nano-drug delivery systems (DDSs) to the brain in order to administer neuro-protective and/or neuro-regenerative agents to the CNS [7].

Unexpectedly, after a traumatic event, the brain parenchyma develops its own healing mechanisms by activating a range of

* Corresponding author.
E-mail address: nunzio.denora@uniba.it (N. Denora).
[1] These authors contributed equally.

https://doi.org/10.1016/j.jddst.2024.105699
Received 28 March 2024; Received in revised form 19 April 2024; Accepted 20 April 2024
Available online 22 April 2024

compensatory phenomena known as neuroplasticity [8]. These processes include adjustments to growth factor signaling, synaptogenesis, angiogenesis, neuron cell proliferation, and cell structural alterations with the goal of enhancing functional recovery [9,10]. According to current scientific findings, neurotrophins revealed a significant role [11] and, among them, the brain-derived neurotrophic factor (BDNF) has been singled out as a potential factor connected to processes of brain tissue repair and regeneration [12,13]. Numerous beneficial events, including neuronal survival, differentiation, migration, synaptogenesis, and plasticity, are influenced by the binding of BDNF to its physiological tropomyosin receptor kinase (TrkB), suggesting several potential advantages [11,14].

Thus, BDNF therapy could be a successful option for post-injury treatment, enabling a potential recovery of the tissue. This point is particularly interesting when considering children who sustain brain injuries; in fact, they should be treated quicker than adults due to the sequelae of impairments generated by an early damage to an immature brain parenchyma. Besides, the lack of effective non-invasive therapeutic treatments complicates the lives of younger patients [15].

Unfortunately, BDNF is a pH-sensitive molecule with poor permeability across the BBB and short half-life, so its administration would require extremely intrusive procedures when using a standard treatment strategy [11,13]. Therefore, using novel nano DDSs to encapsulate and deliver BDNF would circumvent the pharmacokinetic restrictions associated with conventional therapeutics, opening the way for a promising strategy that would enable the handling of secondary neurodegenerative phenomena via more compliant processes [16].

In recent years, the scientific community's focus has been on innovative nanoformulations that, in complex conditions such as the Covid-19 pandemic crisis, have generated a more effective resolution than conventional therapeutical procedures [17]. Similarly, it is interesting to note that nanoformulations also offer a number of advantages for the treatment of pathological conditions that demand a multifaced approach as in the TBI-like situation [18]. Thus, in this vast panorama, solid lipid nanoparticles (SLNs) have attracted interest as they include a number of favorable qualities for brain delivery. More in detail, SLNs would enable the encapsulation of both hydrophilic and hydrophobic compounds that may be incorporated into the lipidic core [19,20]. This property is highly intriguing when considering the delivery of biologicals that require protection from plasmatic degradants before reaching the therapeutic target [16,21]. In addition, SLNs are able to bypass reticuloendothelial system's (RES) absorption when synthesized in a dimensional window between 120 and 200 nm, extending the circulating time and the possibility to arrive safely to the target site without the need for additional surface modifications [22]. Unfortunately, existing bulk production methods are unable to ensure the reliable fabrication of nanosystems with appropriate properties for brain delivery, due to the difficulty to precisely regulate every manufacturing parameter step-by-step [23]. Additionally, it is still very difficult to produce lipid nanosystems incorporating biologicals taking into account the long manufacturing time, the insufficient yield, and the rapid degradation of the compounds while applying traditional working methods [24]. As a consequence, emerging production techniques are needed to resolve the previously stated challenges, rendering feasible to successfully fabricate brain targeted SLNs [25,26].

The microfluidic technique is the most advanced method applied in the production of SLNs [25,27,28], providing clear benefits over conventional practices [24,29]. The main advantages include the decoupling of the process from the operator's dexterity, the replacement of harmful solvents stepping toward a more sustainable approach, time- and cost-effective processes, and the ability to keep accurately regulated the experimental conditions which guarantees great reproducibility and consistency [30,31].

Taking cues from these insights, the objective of this study was to utilize microfluidic technology for the production of BDNF-SLNs specifically tailored for brain delivery, aiming to overcome the pharmacokinetic limitations that hinder the utilization of biologicals in therapy. Building upon a prior study by Sommonte et al. [32], which optimized the *in-flow* preparation of SLNs carrying a model enzyme, we adopted the same protocol. Utilizing a commercially available microfluidic device with herringbone internal geometry allowed us to produce high-quality nanosized SLNs suitable for parenteral administration. We subjected the BDNF-SLNs to characterization and conducted a short-term stability assessment. Furthermore, we performed a haemolysis assay to evaluate the biocompatibility of the microfluidic-based formulation with blood components. To assess the enhanced transport of encapsulated BDNF compared to plain BDNF, we conducted a permeability study using an *in vitro* immortalized human endothelial (hCMEC/D3) BBB model. Lastly, we evaluated the neuroprotective properties of plain BDNF and BDNF-SLNs using an *in vitro* simplified model resembling TBI.

2. Materials and methods

2.1. Materials

All chemicals were the highest purity available and were used as received without further purification or distillation.

Cetyl palmitate was provided by Farmalabor (Italy). Dulbecco's phosphate buffered saline, Lutrol F68 (Poloxamer 188), double-distilled water, and all analytical grade solvents/salts were purchased from Sigma-Aldrich (Italy).

For cellular studies, Transwell® permeable supports were from Corning (Corning, NY, USA). Fetal Bovine Serum (FBS), penicillin (100 U/mL), and streptomycin (100 μm/mL) and all the media and supplements for cell culture were purchased from EuroClone (Italy).

Human brain-derived neutrophic factor (BDNF, carrier free, recombinant, expressed in *E. coli*, suitable for cell culture), human BDNF ELISA kit, Diazepam, Fluorescein isothiocyanate-dextran (FD4), lipopolysaccharide (LPS), the nitrite assay kit (Griess reagent), human serum were purchased from Sigma-Aldrich (Italy).

2.2. Microfluidic-based preparation of SLNs encapsulating BDNF

For the production of BDNF-SLNs, it was selected a commercially available microfluidic device purchased from Microfluidic Chip Shop (Germany). Due to the presence of a modified herringbone design, the generation of SLNs happened due to a nanoprecipitation process caused by the swirling mixing of aqueous phase and organic phase which flowed in the same direction during the microfluidic path. The microfluidic set-up has been engineered using the method previously optimized [32]. Polyethylene syringes placed on syringe pumps were used to inject miscible fluids into the microfluidic chip at a constant flow rate. The organic phase consisted of an ethanolic solution (95 %) with cetyl palmitate (10 mg/mL), while the aqueous phase was prepared using double-distilled water containing Lutrol F68 2 % (w/v). The aqueous solution was filtered using a cellulose-acetate syringe filter measuring 25 mm 0.45 μm (Scharlab S.L., Spain) to prevent the channels from becoming clogged. After, the BDNF was placed inside the aqueous phase at a final concentration 1 μg/mL. During the production, the fluid rate ratio (FRR) was kept at 1: 5 (organic phase: aqueous phase), while the total flow rate (TFR) was accorded to 6 mL/min. Using an infrared lamp (Incandescent 230–250V BR125, 150W E27 IR RE, Philips, Germany) placed at distance of 10 cm from the syringe carrying the organic phase, the organic phase was maintained at a temperature above the melting point of the lipid while the chip was kept in a hot bath (i.e., 60 °C) throughout the procedure. After being produced, the formulation was maintained on a warm stirring plate allowing to facilitate the ethanol evaporation gently balancing at room temperature. Then, the formulation was consolidated for 15 min at 4 °C, followed by the purification phase using centrifuge filters (Amicon® ultra- 15, centrifugal filters ultracel® - 50K, Merck Millipore Ltd., Ireland) to completely remove the

organic solvent and unencapsulated BDNF. The washes with double-distilled water were performed four times at 3500 rpm, 5 min, and 4 °C.

2.3. Dynamic light scattering (DLS) and Z-potential

The size distribution, polydispersity index (PDI), and ζ-potential of the SLNs were evaluated using a Zetasizer Nano ZS (Malvern Instruments Ltd., UK). Approximately 1 mL of a 1:50 diluted solution in double-distilled water of each sample was analyzed using disposable polystyrene cuvettes (Sarstedt AG & Co., Germany) at 25 ± 0.1 °C. The surface ζ-potential of the SLNs was evaluated using a 750 μL of the 1:50 dilution in demineralized water of the nanoparticle suspension in a disposable folder capillary cell (DTS1070, Malvern Instruments Ltd., UK). All the experiments were performed in triplicate and resulting data are shown as the mean ± standard deviation of each triplicate.

2.4. Nanoparticle tracking analysis (NTA)

According to literature [33], the formulations were analyzed in terms of particle size and concentration as SLNs/mL with the NanoSight NS300 (Malvern Panalytical) following the manufacturer's instructions (NanoSight NS300 User Manual, MAN0541-02-EN, 2018). Each sample was diluted 1:1000 in Milli-Q pre-filtered water and then injected at a constant syringe flow (flow rate = 50 μL). Samples were run performing three-60s videos, and then data were collected reporting the mean ± standard deviation of each triplicate.

2.5. Evaluation of encapsulation efficacy (EE %)

The assessment of EE (%) of the formulation was conducted via the direct measurement of encapsulated BDNF. Briefly, 100 μL of BDNF-SLNs were lyophilized and digested using a 500 μL mixture containing chloroform and double-distilled water (1:1 v/v). The amount of BDNF extracted by the aqueous phase was evaluated using BDNF ELISA kit. All absorbance measurements were carried out in triplicate at room temperature, by using a Tecan Infinite® 200 PRO plate reader (Tecan, Switzerland).

The EE % was calculated using Eq. (1) [32].

$$\text{EE}\ (\%) = \frac{\text{mass of drug found into SLNs}}{\text{mass of drug initially added}} \times 100 \qquad \text{Eq. (1)}$$

2.6. In vitro release studies

The *in vitro* release experiment was conducted using Franz-diffusion cells as reported previously [19,32]. More in detail, the experiments were carried out in presence and in absence of lipase from porcine inside the donor compartment. The BDNF-loaded SLNs were positioned on an artificial cellulose acetate membrane diffusion barrier (area of 0.6 cm^2, 50 kDa, Fisher Scientific, Italy), which divides the donor and receptor compartments. In this study, 400 μL of BDNF-loaded SLNs (at a concentration of 1,03 ng/mL in terms of BDNF) were placed in the donor compartment and diluted with 500 μL of water or lipase (1 mg/mL into double-distilled water) to allow the degradation of the SLNs' lipidic matrix [26]. In both cases, the receptor compartment contained PBS (pH 7.4) as relevant medium, while the entire systems were maintained at a temperature of 37 ± 0.5 °C. At certain time points (0, 2, 4, 8, 24, 48, and 72 h), 200 μL of receptor phase was taken and replaced with 200 μL of warm PBS to preserve *sink* condition. The released BDNF of each sample was quantified by BDNF ELISA kit. Each experiment was performed in triplicate.

2.7. Short-term physical stability study

Short-term stability study was performed on both empty and BDNF-SLNs by evaluating the size and PDI in different media (i.e., PBS (pH = 7.4) and human serum). In detail, 200 μL of each formulation was dispersed in 1.5 mL of the above-mentioned media and incubated at 37 °C, under magnetic stirring in order to simulate physiological conditions. At predetermined time points (5, 10, 15, 30, 60, 90, and 120 min) an aliquot of 20 μL of the sample was withdrawn and diluted in double distilled water to be analyzed by Zetasizer Nano ZS (Malvern Instruments Ltd., UK). The results were expressed as mean ± standard deviation.

2.8. Haemolysis assay

In vitro haemolysis assay of BDNF-SLNs and empty SLNs was performed using human whole blood (HWB) kindly donated by a healthy volunteer. HWB was freshly diluted before the test as follows: 0.556 μL of HWB was added to 1.944 mL of sterile Dulbecco's PBS pH 7.4 gently shaking. 1 mL of this suspension was withdrawn and added to 49 mL of sterile Dulbecco's PBS pH 7.4. For the assay, 50 μL of each formulation at several lipid content concentrations, namely 0.10, 0.020, 0.002, and 0.0002 mg/mL of both empty and BDNF-SLNs, was added to 950 μL of the before-diluted blood. After addition, the mixtures were continuously shaken using a thermomixer C (Eppendorf) at 300 rpm, 37 °C for 2 h and thereafter further mixed by inversion every 15 min. Subsequently the incubation, the mixtures were centrifuged at 503×*g* for 5 min at 5 °C [34].

Following, the supernatants were analyzed via UV-spectrometry at a λ = 420 nm using a Multiskan SkyHigh Microplate Spectrophotometry (ThermoFisher Scientific).

Values were referred to a Triton X-100 (1 % w/v) used as 100 % reference of haemolytic activity (positive control). The negative control was prepared by incubating 50 μL of sterile Dulbecco's PBS (pH 7.4) and 950 μL of diluted blood.

The extent of haemolysis as a percentage (% H) was calculated applying Eq. (2) as reported in literature [35].

$$\text{H}\ (\%) = \frac{\left(Abs_{\ Test} - Abs_{\ Neg}\right)}{\left(Abs_{\ Pos} - Abs_{\ Neg}\right)} \times 100 \qquad \text{Eq. (2)}$$

where:

Abs Test is the absorbance of the test sample, Abs Neg is referred to as negative control, and Abs Pos is the absorbance of positive control [35].

2.9. In vitro BBB model

hCMEC/D3 cells were kindly provided by Pierre-Olivier Couraud (Universitè Paris Descartes, Paris, France). As reported in literature [19,36], cells between passages 25 and 35 were grown for 15 days in EndoGRO medium nourished with EndoGRO MV supplement kit, 10 % FBS, basal FGF (200 ng/ml), penicillin–streptomycin (1 %), lithium chloride (10 mM) and resveratrol (10 μM) and kept at 37 °C with 5 % CO_2.

To create the *in vitro* model of BBB, the cells (21,000 cells/cm^2) were seeded on the apical side of Transwell® insert (polyester 24-well, 0.4 μm pore size, insert 6.5 mm), precoated with Collagen type I (1 %). The medium (100 μL in the apical compartment, and 600 μL in the basolateral compartment) was changed every 2–3 days and the cell monolayer was monitored. The constitution of tight junctions between cells was tracked by measuring the transendothelial electrical resistance (TEER) using EVOM apparatus [37].

2.10. Endothelial permeability of BDNF-SLNs

At 15th day after seeding, 100 μL of PBS-suspended BDNF (3.98×10^{-3} μg/mL), BDNF-SLNs (3.98×10^{-3} μg/mL drug concentration; 0.6 mg/mL of lipid concentration), empty SLNs (0.6 mg/mL of lipid concentration), Diazepam (75 μM), and fluorescein isothiocyanate-dextran

(FD4) (200 μg/mL) were added to the apical compartment of hCMEC/D3 cell culture system. After 3 h, samples from basolateral compartments were collected. The endothelial permeability (P_{app}) of BDNF, BDNF-SLNs, Diazepam, and FD4 were calculated following Eq. (3) as reported in literature [37].

$$P_{app} = \frac{V_a}{(\text{area } x \text{ time})} \; x \; \frac{Drug\ acceptor}{Drug\ initial} \qquad \text{Eq. (3)}$$

Where:

"Va" is the volume in the apical compartment (mL); "area" is the total area of the insert (cm^2); "time" is the total transport time (sec); "Drug acceptor" is the amount of drug in the basolateral compartment; "Drug initial" is the drug added in the apical compartment.

The quantification of Diazepam was performed by HPLC method, as reported in literature [38], using Agilent 1260 Infinity quaternary LC VL system equipped with a variable wavelength detector and with OpenLab DCS software. Briefly, a C18 ODS 5-μm HyperClone column (120 Å, 250x4.6-mm) (Phenomenex, Italy) was used. The mobile phase consisted of a mixture methanol: water in a ratio 75:25 (v/v). Column temperature was 35 °C, and the mobile phase flow was set at 1.1 mL/min. Each sample was run for 8 min, and it was injected with 30 μL. Absorbance was recorded at λ = 254 nm.

The quantification of FD4 was performed by recording the spectra of absorbance (λ = 495 nm) and emission (λ = 520 nm) using a spectrophotometer (Infinite® 200 PRO, Tecan, Switzerland).

2.11. BDNF quantification by ELISA analysis

The quantity of BDNF was evaluated by using the human BDNF ELISA kit as defined by the Sigma-Aldrich protocol. Briefly, all reagent and samples were used at room temperature. The appropriate solvent (Diluent B) was used to dilute each sample, and then 100 μL of each dilution was poured into one well. The system was incubated at room temperature for 150 min while being gently shaken. After the time required, the solutions were discarded, and each well was washed four times by using the wash solution (1x). Then, 100 μL of a 1x detection antibody was put into each well, and the mixture was allowed to sit for 60 min while being gently shaken at room temperature. After, each well has been washed four times with the wash solution (1x). Subsequently, 100 μL of prepared Streptavidin solution was added into each well, incubating for 45 min at room temperature. The solutions were discarded, and the washes were repeated. Then, 100 μL of TMB-One step substrate reagent was added to each well, incubating for 30 min in the dark at room temperature with gently shaking. 50 μL of Stop solution was poured into each well and absorbance was read immediately at λ = 450 nm using a spectrophotometer (Infinite® 200 PRO, Tecan, Switzerland). Each analysis was performed in triplicate, and the resulting data were reported as mean ± standard deviation of each triplicate.

2.12. N9 cell culture growth and treatment

The N9 cell line is commonly used in neuroscience research as a model for microglial cells. In this case, the N9 cells were cultured in DMEM/F12 medium (Gibco 11320033) supplemented with inactivated FBS (Gibco 10270, inactivated at 56 °C for 30 min), 2 mM L-glutamine (Biowest X0550), and penicillin-streptomycin (Gibco 15070063). The cells were maintained at a temperature of 37 °C with a 5 % CO_2 atmosphere in a humidified incubator. After reaching confluence, the cells were detached with 0.125 % Trypsin (Gibco 25200) for 5 min at 37 °C, followed by inactivation with complete medium. The pellet was collected by centrifugation at 200×*g* for 5 min at room temperature. Treatments were conducted 24 h after new seeding, which was performed in triplicate in 24 multi-well plates, seeding 100,000 cells per well. The concentrations used for treatments were as follows: LPS 1 μg/ml, IFN-γ 0.1 μg/mL (in a mix with LPS), BDNF 25 ng/mL and BDNF-SLNs 25 ng/mL.

2.13. Real-time PCR

After 24 h from the addition of the treatments, total RNA was isolated from the samples using the commercially available kit Qiagen RNeasy Mini Kit (Cat. No. 74104), according to the manufacturer's instructions, by directly lysing the cells in the multiwells. RNA quality and quantity were assessed using a NanoDrop spectrophotometer. cDNA was synthesized using QuantiTect Reverse Transcription Kit (Cat. No. 205311). Real-time PCR was performed using Applied Biosystems TaqMan™ Gene Expression Master Mix (catalog number: 4369016) and the QuantStudio™ 3 Real-Time PCR System (Applied Biosystems). The mix of primers and probes for *Nos2* and housekeeping gene (*Actb*) were purchased from Integrated DNA Technologies. The real-time PCR reaction mixture was prepared according to the user guide of the TaqMan™ master mix relative to the 96 fast-plate duplex setup. The thermal cycling conditions were as follows: 50 °C for 2 min, 95 °C for 10 min, and 40 cycles of 95 °C for 15 s and 60 °C for 1 min. The real-time PCR data were analyzed using the $2^{-\Delta\Delta Cq}$ method. The results were expressed as mean (log_{10}) ± standard deviation.

2.14. Measurement of nitrite (NO^{2-}) levels

The level of nitrites produced after the neuroinflammatory damage was evaluated by using the commercially available nitrite assay kit (Griess reagent) purchased from Sigma-Aldrich. After 24h of treatment, the media of the samples were collected and were used to assess the amount of nitrites (NO^{2-}) which is a stable NO product. Tests were performed by mixing 100 μL of each sample with 10 μL of Griess reagent I, 10 μL of Griess reagent II and 80 μL of nitrite buffer. The nitrite concentration was evaluated after 10 min of incubation by measuring the absorbance at λ = 540 nm using using a spectrophotometer (Infinite® 200 PRO, Tecan, Switzerland). The measurement was performed in triplicate and data are shown as mean ± standard deviation.

2.15. Statistical analysis

Data have been presented when needed as a mean value ± standard deviation value. All data were obtained in triple replicates unless stated otherwise. When comparing data sets for statistical significance, one-way ANOVA analysis, Multiple *t*-test, and Student t-test were performed (Version GraphPad Prism 8.0.2), adhering to a p value of ≤ 0.05.

3. Results and discussion

3.1. Microfluidic-assisted production and characterization of BDNF-SLNs

For the production of BDNF-SLNs was applied a commercially available polycarbonate device. The chip is characterized by an internal staggered herringbone pattern and a Y-shaped geometry with two inlets converging into the main channel (Fig. 1). This device was chosen in accordance with the required output as the miniaturized microchannels are responsible for the high-quality result. In fact, in the case microfluidic-assisted production conducted under laminar flow condition, the focus is on diffusive phenomena which guide the chemical reactions at the interfaces of the two fluids by following the Fick's law [39].

It is interesting to note the abundance of studies in literature showing how effectively the herringbone structure ensures the creation of nanosized monodisperse nanoformulations [24,40]. Since the chaotic aversion phenomena occurs at intermediate Reynolds numbers, the proposed shape allows for the production of rotational flow conditions. Under these circumstances, the flow direction within the device is changed numerous times, reducing the time required for molecules to

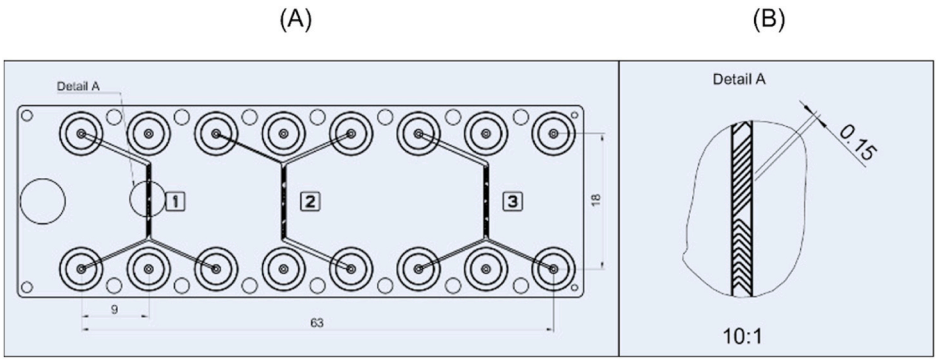

Fig. 1. Schematic representation of the microfluidic set-up and of the Y-shaped microfluidic device [42].

diffuse and enabling faster production with a high degree of monodispersion while keeping all the parameters strictly controlled [41].

In a more detailed way, the *in-flow* production of BDNF-SLNs was carried out on using the previously published set-up [32] with slight changes (Fig. 1). Specifically, the BDNF was solubilized in a surfactant aqueous solution (Lutrol F68, 2 % w/v) at a final concentration of 1 μg/mL, while the organic phase consisted of cetyl palmitate in ethanol (95 %, 10 mg/mL).

Here, in contrast to prior work [32], the novel device with smaller microchannel dimensions necessitated a change in the flow parameters to prevent chip leakage. As a result, the production was conducted at a TFR of 6 mL/min while maintaining the previously optimized FRR of 1:5 between the organic phase and aqueous phase.

Characterization data of the BDNF-SLNs showed the technique's robustness and proficiency in generating appropriate nanosystems in terms of size and PDI. According to DLS analyses, the formulations revealed good findings regarding hydrodynamic dimensional range (190.3 ± 10.1 nm) and PDI (0.180 ± 0.023), and the EE % (40.3 ± 2.7 %). It is important to emphasize that an EE of 40 % of the total load is consistent with other encapsulated biological molecules when taking into account other microfluidic-based SLNs [43]. Indeed, in contrast to small compounds, biotechnological molecules' three-dimensional structure, and spatial arrangement of hydrophobic amino acid residues may have a significant impact on the lipid matrix's deposition and, consequently, affecting the amount of encapsulated cargo. In contrast to prior work in which the presence of the biological molecule had been demonstrated both inside the lipid matrix and adsorbed on the surface of the nanosystem resulting in a major EE % [32], here Z-potential values of empty and BDNF-loaded SLNs were found to be stable and negative, respectively (– 38.3 ± 1.18 mV) and (– 39.2 ± 1.30 mV), giving precious information about the placement of the drug only within the lipidic core. The BDNF is a protein characterized by an isoelectric point at pH 9.6 [44] and considering the aqueous Lutrol F68-stabilized solution (2 % w/v) at the pH value of 6.30, all the polarized groups of BDNF were protonated when it was inside the aqueous phase. The evidence that BDNF-SLNs exposed a homogeneous negative surface charge was indicative that the growth factor was localized within the lipid core, and not absorbed on the nanosystems' surface; otherwise, the ζ-potential values would have been turned positive [32]. To conclude, it should be reiterated that there are works in which a higher EE has been obtained [45], however these examples do not concern microfluidic-based lipid formulation. Furthermore, a 40 % EE serves as suitable starting point for further biological investigations, since the *in vitro* neurotrophic activity of BDNF has been tested in a range of concentration between 10 and 100 ng/mL [46,47].

In addition to characterization data, NTA analysis confirmed the DLS results, highlighting the actual size of moving BDNF-SLNs equal to 166.5 nm (±53.8 nm), with a concentration of $9.31e^{+008}$ ($\pm 7.68e^{+006}$) particles/mL (Fig. 2).

The BDNF-SLNs release study was achieved via the use of Franz-diffusion cell using PBS as receptor medium at 37 °C to mimic physiological condition. As broadly reported in literature, the SLNs are a valuable drug delivery system performing a sustained release of the encapsulated cargo over time after enzymatic degradation of the lipid matrix [22]. For this reason, the *in vitro* release experiment was conducted with and without lipase in the donor compartment in order to simulate a more physiological sitting and stimulating the degradation of the lipidic matrix [26]. As shown in Fig. 3, BDNF-loaded SLNs in presence of water in the donor compartment reached a release of the 20 % in the first 4 h of incubation and remained steady within 72 h.

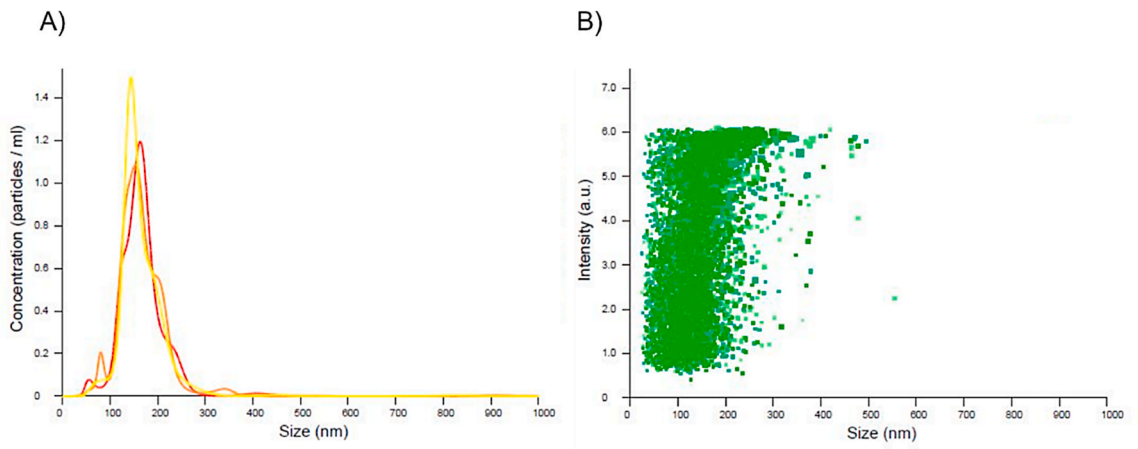

Fig. 2. Size distribution from NTA measurements of BDNF-SLNs using constant experimental and evaluation parameters. A) Triplicate measurements of the same monodisperse sample size vs. concentration was reported. **B**) Triplicate measurements of the same monodisperse sample size vs. intensity was reported.

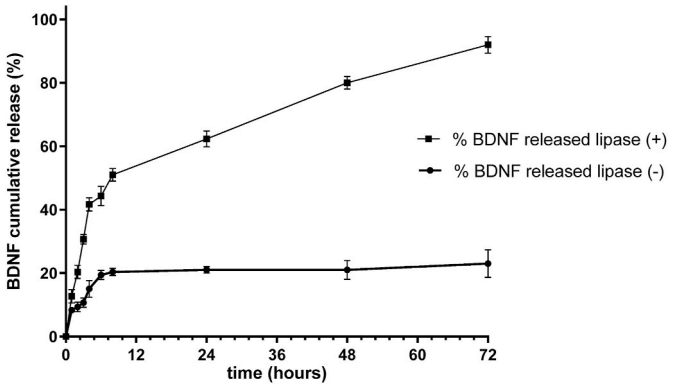

Fig. 3. *In vitro* release profiles of BDNF from SLNs using Franz-diffusion cell at 37°C. The study was performed diluting BDNF-loaded SLNs with the same amount of water or lipase (1 mg/mL in water) in the donor compartment. Resulting data were reported as mean ± SD, n = 3.

Comparatively, under lipase-positive conditions, BDNF was released from the lipid matrix to the extent of 40 % in the first 4 h, 64 % in the next 24 h, and 93 % up to 72 h.

3.2. Cellular permeability study through the in vitro BBB model

To assess the permeability of both plain and encapsulated BDNF through the barrier, the *in vitro* BBB model was constructed in accordance with the literature [19,36]. The hCMEC/D3 monolayer is an adequate model able to accurately replicate the human BBB physiological condition as it shows a good representation of the majority of the receptors and transporters expressed *in vivo*, while enabling relevant CNS cellular and molecular drug transport pathways [36].

The cell culture was built using Transwell® set-up in which a monolayer of hCMEC/D3 was seeded on a porous insert, determining the formation of an apical compartment and a basolateral one which represented the "blood" side and the "brain" side, respectively.

To control the viability of the *in vitro* model [37], TEER values were checked during the formation of hCMEC/D3 monolayer. TEER values increased from 134.2 ± 3.4 Ω (1 day after seeding) to 172.9 ± 2.7 Ω (on the day 15th after seeding).

The permeability study was conducted by evaluating the permeability of plain BDNF, BDNF-SLNs, diazepam and FD4 across the cell monolayer. The experiment was carried out by using the same concentration of plain BDNF and BDNF loaded into SLNs, namely 3.98×10^{-3} μg/mL, while the lipid content of BDNF-SLNs and empty SLNs was 0.6 mg/mL. To evaluate the transcellular permeability was used diazepam at final concentration of 75 μM, while for the paracellular pathway was applied FD4 at 200 μg/mL. The permeation across the monolayer of hCMEC/D3 was estimated after 3 h of incubation by measuring the amount of BDNF, diazepam and FD4 collected in the basolateral compartment. The P_{app} was calculated following Eq. (3) [37], evaluating values for plain BDNF, BDNF-SLNs, diazepam, and FD4 (Fig. 4).

After 3 h of permeation across the cell monolayer, collected data demonstrated a slight increase in the P_{app} of the encapsulated BDNF ($1.27x\ 10^{-5}$ cm/s) in comparison with plain BDNF ($9.31\ x\ 10^{-6}$ cm/s) at the same concentration.

As documented in literature [19,48], the SLNs demonstrated to be a valuable nano DDSs, also considering the great protection of the cargo provided by the lipid core from the rapid *in vivo* degradation. In addition, the coating of the nanosystems with a surfactant would create a steric hindrance, slowing the opsonization process and the rapid clearance from the RES. The improved SLNs retention in brain capillaries combined with adsorption onto capillary walls may result in a higher concentration gradient, which would improve drug delivery to the brain by improving transport across the endothelial cell layer [16]. These pharmacokinetic properties allow the SLNs to arrive unmodified to the site of interest, where internalization takes place mainly exploiting the mechanism of clathrin-mediated endocytosis. After the uptake, the nanosystem could take the lysosomal or endosomal route. In the former situation, the lipid matrix degrades, resulting in drug release into the cell, whereas the endosome transports the entire nanosystem to the opposite pole of the barrier, leading the release of embedded drug in the brain compartment [48].

In the present study the permeability of BDNF encapsulated within SLNs resulted greater than plain BDNF in a well-established model reflecting the actual situation of a healthy barrier. Concerning a TBI-compromised condition, however, the dysregulation of tight junctions and extracellular matrix is responsible for the increase in paracellular permeability [3], thus highlighting the possibility that using a pathological-like model the SLNs permeability and the release of encapsulated drug could be increased even more.

A)

Sample	P_{app} (cm/sec)
BDNF	9.31×10^{-6}
BDNF-loaded SLNs	1.27×10^{-5}
Diazepam	4.61×10^{-5}
FD4	1.60×10^{-5}

B)

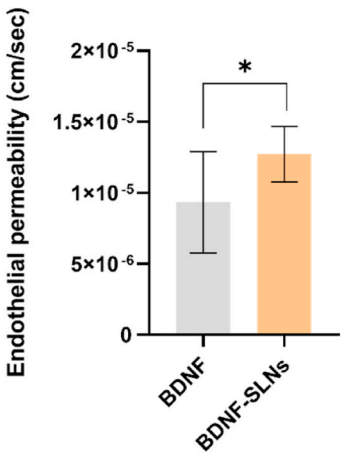

Fig. 4. Endothelial permeability of plain BDNF, BDNF-SLNs, diazepam and FD4. (**A**) Summary of calculated values of P_{app} after 3 h of incubation in the Transwell® system. (**B**) Graphical illustration of endothelial permeability study results by comparing plain BDNF and BDNF-SLNs. Experiments were performed in triplicate and reported as mean ± standard deviation. Student *t*-test was performed to calculate the statistical significance of plain BDNF and BDNF-SLNs, adhering to a p value of ≤0.05 [* = $p < 0.0332$ by Student *t*-test.].

3.3. Haemolysis assay

After delivery, nanoparticles can interact with blood components, causing various blood phenomena including the breakdown of blood clotting pathways, complement activation, and erythrocyte haemolysis. Indeed, preclinical studies on red blood cell compatibility are essential in assessing the safety of both the carrier and the drug to be administered [49,50]. The *in vitro* haemolysis assay is used to determine the amount of hemoglobin released from erythrocyte breakdown after exposure to nanoparticles. In the presence of oxygen, hemoglobin quickly converts to oxyhemoglobin, which is then quantified spectrophotometrically. Following the assay, the formulations are classified as non-hemolytic when the percentage of hemolysis is less than 5 %, and certainly hemolytic when the range is larger than 25 % [51].

To evaluate the biocompatibility of empty and BDNF-SLNs with blood components in the context of potential parenteral administration of these nanocarriers, a hemolysis test simulating the interaction between nanocarriers and whole blood was conducted (Fig. 5). Data have been reported as haemolysis percentage (H %) in comparison with the positive control Triton X-100 1 % (w/v) and the blank/negative control PBS which were used for complete haemolysis (100 %) and zero haemolysis (0 %, not shown in Fig. 5), respectively.

The haemolytic activity of the formulations is purely related to the carrier and not to the presence of BDNF since the behavioral trend of empty SLNs and BDNF-SLNs is alignable. To our knowledge, no available data have been published about haemolytic activity of microfluidic-based SLNs. When examined at the production concentration in terms of lipid and surfactant content (0.10 mg/mL), both empty SLNs and BDNF-SLNs showed a modest rate of haemolysis, respectively 7.80 ± 0.08 and 8.10 ± 0.05 %. From this perspective, it may be possible to explain the higher haemolysis percentage of the formulations at the same concentration as they are produced, requiring further dilutions before their administration. Interestingly, when alternative formulation dilutions were tried, however, the haemolysis percentage decreased by less than 5 %, showing that the formulations were non-haemolytic [52,53].

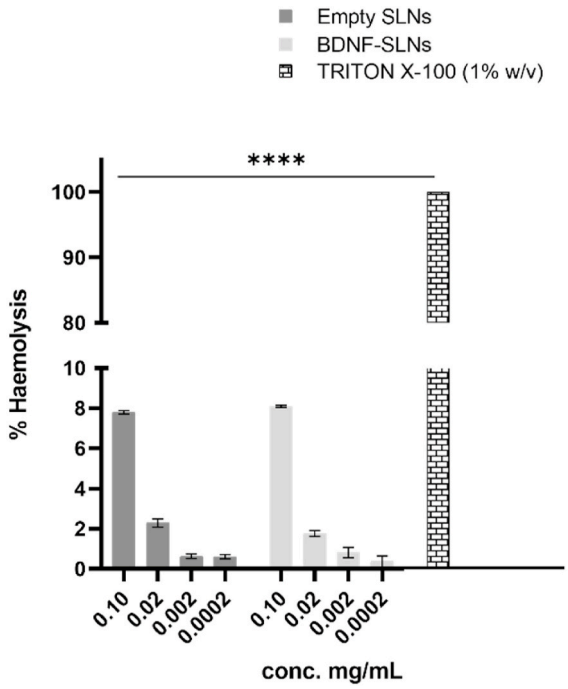

Fig. 5. Haemolysis test results after incubation of empty SLNs and BDNF-SLNs with HWB. Data have been shown as mean ± standard deviation. One-way ANOVA was used to calculate statistical significance of the empty SLNs and BDNF-SLNs versus the positive control [ns = p value > 0.05; * = p < 0.0332; ** = p value < 0.0021; *** = p value < 0.0002; **** = p value < 0.0001]. All samples revealed a statistical significance (****) compared to the Triton X-100 (1 % w/v).

3.4. Short-term physical stability study

As reported in the literature, stability studies of both empty and enzyme loaded SLNs have been previously conducted in PBS and human serum [25,32]. The same microfluidic technique used to produce the latter SLNs was also employed for the production of BDNF-SLNs. To the best of our knowledge, previous evaluation regarding the colloidal stability of BDNF-SLNs produced via microfluidic technique have not been found. Therefore, a short-term stability study was assessed on empty SLNs and BDNF-SLNs, in both above mentioned media (i.e., PBS and human serum). Resulting data have been shown in Fig. 6 and revealed that, considering PBS as relevant medium, there was no significant increase in size and PDI for empty SLNs and those encapsulating BDNF after the observation time of 120 min (p-value ns). As reported in literature, the SLNs represent a more stable DDSs due to the presence of the lipid core, showing limited phenomena of aggregation and surfactant expansion over time when tested in PBS [43]. Conversely, the stability test performed in human serum revealed the growing trend in terms of size and more specifically in PDI for both evaluated SLNs ($p < 0.05$; $p < 0.0001$). This phenomenon could be ascribable to the protein corona effect [54], which usually occurs when a nanocarriers circulates in the physiological fluids, due to the presence of biological substances, mostly proteins, in the human plasma. Here, since we have emulated the physiological conditions by investigating the stability in human serum, the increasing pattern was explained by the dynamic adsorption-desorption phenomena involving both BDNF and serum proteins on the surface of BDNF-SLNs.

3.5. In vitro neuroinflammation study

As previously mentioned, when TBI occurs the BBB suffers both acute and delayed impairments. First of all, the primary injury induces changes in the molecular traffic in and out the brain compartment and the usual functional relations between glial cells and the cerebrovascular endothelium are altered [3,6]. Subsequently, the injury results in oxidative stress, which boosts the production of proinflammatory mediators and the expression of cell adhesion molecules on the surface of the brain endothelium, also allowing inflammatory cells to enter the injured brain parenchyma [6]. The neuro-inflammatory event typically starts after the initial injury in the form of microglial and complement activation, which is in charge of repairing the injured cells and providing defense against encroaching pathogens [55]. Additionally, complement activation increases the BBB-crossing of neutrophils, monocytes, and lymphocytes, which release prostaglandins, chemokines, and cell adhesion molecules [56,57].

At the same time, the microglial activation triggers the activation of iNOS that consequences in NO production [58]. Excessive production of NO by iNOS can lead to the formation of highly reactive nitrogen species that can cause oxidative stress, damaging cellular components like proteins, lipids, and DNA [59]. Oxidative stress is a major contributor to neurodegenerative damage, in fact the prolonged and sustained production of NO, especially at high concentrations, may trigger neuronal cell death through mechanisms such as apoptosis or necrosis. As a result, the delayed onset secondary phase of the disease is responsible for long-term damages caused by neuroinflammation and no therapies are currently available to revert this detrimental situation [13,15].Several research in literature have shown the possibility to mimic a neuroinflammatory damage-like phenotype using LPS or a mixture of LPS and IFN-γ, which effect is to induce microglial activation leading to an increased expression of *Nos2*, the iNOS gene [60]. To this end, LPS and LPS + IFN-γ mix are applied to a N9 cell line to mimic a neuroinflammation-like condition for evaluating the potential

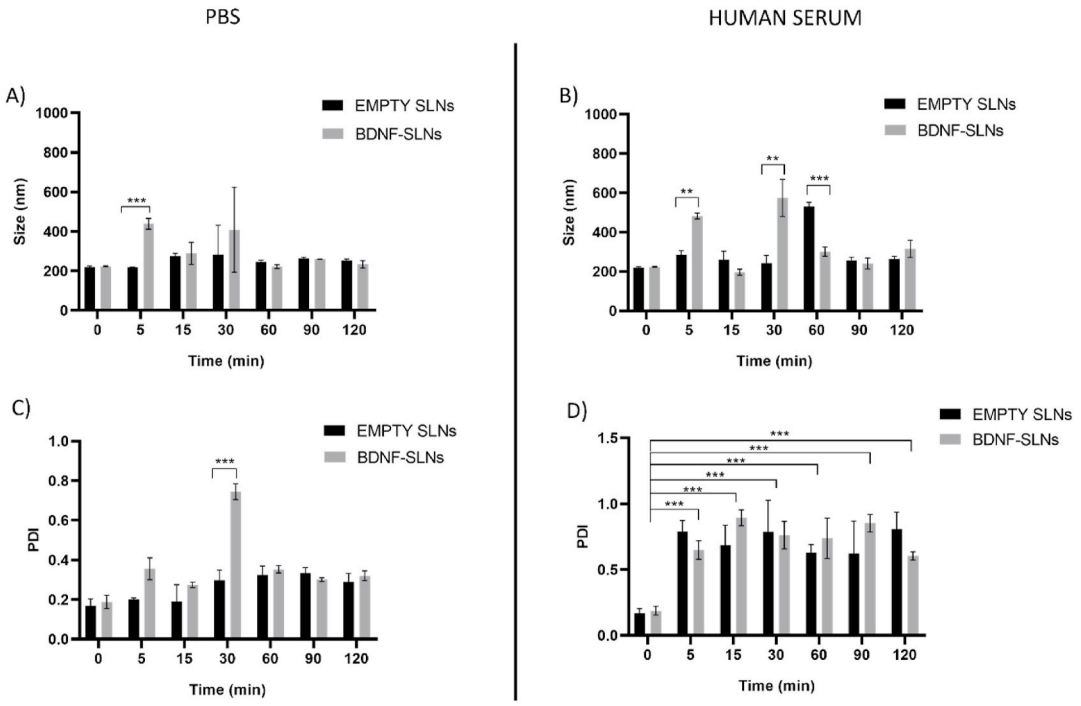

Fig. 6. Short-term stability study of empty and BDNF-SLNs. (**A**) Size of empty and BDNF-SLNs in PBS, (**B**) size of empty and BDNF SLNs in human serum, (**C**) PDI of empty and BDNF-SLNs in PBS, (**D**) PDI of empty and BDNF SLNs in human serum. Results are expressed as mean ± standard deviation. Statistical analysis was performed by a Multiple *t*-test (ns = p-value>0.05; **p < 0.05; ***p < 0.0001).

therapeutic benefits of BDNF. To compare the activity of encapsulated and plain BDNF as neuroprotective agents, a pre-incubation of the cell line with both BDNF-SLNs and plain BDNF, at the same concentration of 25 ng/mL, was carried out for 4 h. Subsequently, LPS alone and a mixture of LPS and IFN-γ (L + I) were added to the cell cultures for a duration of up to 24 h. The levels of *Nos2* mRNA and the amount of nitrites in cell culture media as NO products were then measured to assess the neuroprotective effects of BDNF. The N9 cells that underwent pretreatment with BDNF-SLNs for 4 h before the insult with LPS and L + I show a significant reduction in *Nos2* mRNA levels when compared to plain BDNF and, more prominently, when compared to LPS and L + I control (Fig. 7- **A** and **B**). This is also reflected in the nitrite levels in the cell culture medium of cells pretreated with BDNF-SLNs, which are significantly lower than the nitrite levels in the medium of cells treated only with LPS or L + I (Fig. 7- C and **D**). Data from this experiment clearly showed that the formulation of BDNF-SLNs was capable to reduce nitrites production. In fact, it has been demonstrated that encapsulated BDNF had a substantially greater ability to block iNOS activation than plain BDNF since BDNF alone has a short half-life due to its susceptibility to quick enzymatic degradation, whereas lipid nanocarrier was able to protect the drug enclosed into the lipid core and potential provided sustained release over time. This meant that encapsulated BDNF did not degrade quickly and maintained more its neuroprotective effect, resulting in better outcomes than treatment with the unencapsulated one.

4. Conclusion

In a time where the development of novel formulations for the administration of biological drugs is of paramount importance, we stand at a remarkable crossroads. These formulations hold the potential to revolutionize the treatment of many diseases that have thus far remained intractable. In the case of TBI and other neuro-inflammatory disorders, the absence of effective therapeutic procedures continues to pose a significant challenge. Based on these compelling findings, we selected SLNs as the vehicle for delivering BDNF to the brain. In contrast, traditional SLNs production methods apply not-sustainable solvents, resulting in significantly longer manufacturing times and less effective returns. Furthermore, the importance of the microfluidic approach stems from its ability to scale up the process of fabrication, which connects academic scientific research to the reality of industrial production. Building on a previously refined approach, we created BDNF-loaded SLNs using commercially available equipment and microfluidic technology. The success of our continuous in-flow manufacturing approach was clearly established, as evidenced by the characterization data of BDNF-SLNs. Moreover, our BDNF-SLN formulation proved to be adequately stable in the media where short-term stability was assessed. A haemolysis test demonstrated, for the first time to our knowledge, the biocompatibility of SLNs produced through microfluidics. The *in vitro* permeability study revealed that BDNF encapsulated within SLNs exhibited enhanced permeability compared to free BDNF. Additionally, the neuro-inflammation test conducted on a TBI-like model showed that encapsulated BDNF outperforms the free drug in terms of neuroprotective effects, paving the way for potential advancements in non-invasive treatments.

CRediT authorship contribution statement

Federica Sommonte: Writing – review & editing, Writing – original draft, Project administration, Methodology. **Ilaria Arduino:** Writing – original draft, Methodology, Investigation. **Rosa Maria Iacobazzi:** Investigation, Data curation. **Luna Laera:** Resources, Investigation. **Teresa Silvestri:** Methodology, Investigation. **Angela Assunta Lopedota:** Writing – review & editing, Supervision. **Alessandra Castegna:** Validation, Data curation. **Nunzio Denora:** Writing – review & editing, Supervision, Project administration.

Declaration of competing interest

The authors declare that they have no known competing financial interests or personal relationships that could have appeared to influence the work reported in this paper.

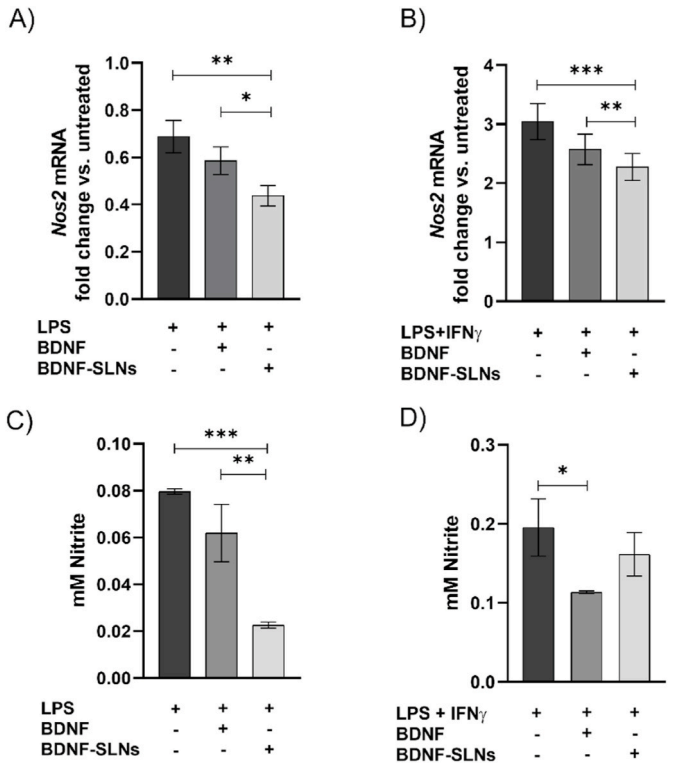

Fig. 7. ***Nos2*** **mRNA expression and nitrite levels after treatment with LPS, LPS + IFN-γ, plain BDNF and BDNF-SLNs.** N9 cells were pre-treated with plain BDNF and BDNF-SLNs for 4 h, then it was added the insult up to 24 h. **(A–B)** *Nos2* mRNA expression after treatment with LPS (**A**) and LPS + IFN-γ (**B**). **(C–D)** Nitrite levels developed after the treatment with LPS (**C**) and LPS + IFN-γ (**D**). Each condition tested was performed in triplicate and the results are presented as the mean ± standard deviation. Student's t-test (*Nos2* mRNA analysis) and ordinary one-way ANOVA (nitrite levels) were conducted to compare the means among the different groups (ns = p value > 0.05; * = p < 0.05; ** = p value < 0.005; *** = p value < 0.0005).

Data availability

Data will be made available on request.

Acknowledgements

Authors acknowledge the University of Bari Aldo Moro (Italy) for its financial support. This work was also supported by #NEXTGENERATIONEU (NGEU) and funded by the Ministry of University and Research (MUR), National Recovery and Resilience Plan (PNRR) Missione 4 Componente 2 Investimento 1.3 "Partenariati estesi alle università, ai centri di ricerca, alle aziende per il finanziamento di progetti di ricerca di base", project MNESYS (PE0000006) - A Multiscale integrated approach to the study of the nervous system in health and disease.

References

[1] F. Sommonte, I. Arduino, G.F. Racaniello, A. Lopalco, A.A. Lopedota, N. Denora, The Complexity of the blood-brain barrier and the Concept of Age-related brain targeting: challenges and potential of novel solid lipid-based formulations, J Pharm Sci 111 (2022) 577–592, https://doi.org/10.1016/j.xphs.2021.08.029.
[2] A.J. Schneier, B.J. Shields, S.G. Hostetler, H. Xiang, G.A. Smith, Incidence of Pediatric traumatic brain injury and associated hospital resource utilization in the United States, Pediatrics 118 (2006) 483–492, https://doi.org/10.1542/peds.2005-2588.
[3] A. Chodobski, B.J. Zink, J. Szmydynger-Chodobska, Blood-brain barrier pathophysiology in traumatic brain injury, Transl Stroke Res 2 (2011) 492–516, https://doi.org/10.1007/s12975-011-0125-x.
[4] M.J. McGinn, J.T. Povlishock, Pathophysiology of traumatic brain injury, Neurosurg. Clin. 27 (2016) 397–407, https://doi.org/10.1016/j.nec.2016.06.002.
[5] L. Han, C. Jiang, Evolution of blood–brain barrier in brain diseases and related systemic nanoscale brain-targeting drug delivery strategies, Acta Pharm. Sin. B 11 (2021) 2306–2325, https://doi.org/10.1016/j.apsb.2020.11.023.
[6] A.A. Ladak, S.A. Enam, M.T. Ibrahim, A review of the molecular mechanisms of traumatic brain injury, World Neurosurg 131 (2019) 126–132, https://doi.org/10.1016/j.wneu.2019.07.039.
[7] B.A. Bony, F.M. Kievit, A role for nanoparticles in treating traumatic brain injury, Pharmaceutics 11 (2019), https://doi.org/10.3390/pharmaceutics11090473.
[8] S.G. Kernie, J.M. Parent, Forebrain neurogenesis after focal Ischemic and traumatic brain injury, Neurobiol. Dis. 37 (2010) 267–274, https://doi.org/10.1016/j.nbd.2009.11.002.
[9] K.M. Schoch, S.K. Madathil, K.E. Saatman, Genetic manipulation of cell death and neuroplasticity pathways in traumatic brain injury, Neurotherapeutics 9 (2012) 323–337, https://doi.org/10.1007/s13311-012-0107-z.
[10] D.G. Stein, S.W. Hoffman, Concepts of CNS plasticity in the context of brain damage and repair, J. Head Trauma Rehabil. 18 (2003), https://doi.org/10.1097/00001199-200307000-00004.
[11] P.H. Lin, L.T. Kuo, H.T. Luh, The roles of neurotrophins in traumatic brain injury, Life 12 (2022), https://doi.org/10.3390/life12010026.
[12] J.G. Boyd, T. Gordon, Neurotrophic factors and their receptors in axonal regeneration and functional recovery after peripheral nerve injury, Mol. Neurobiol. 27 (2003) 277–323, https://doi.org/10.1385/MN:27:3:277.
[13] D. Gustafsson, A. Klang, S. Thams, E. Rostami, The role of bdnf in experimental and clinical traumatic brain injury, Int. J. Mol. Sci. 22 (2021), https://doi.org/10.3390/ijms22073582.
[14] C. Géral, A. Angelova, S. Lesieur, From molecular to nanotechnology strategies for delivery of neurotrophins: emphasis on brain-derived neurotrophic factor (BDNF), Pharmaceutics 5 (2013) 127–167, https://doi.org/10.3390/pharmaceutics5010127.
[15] M.C. Dewan, N. Mummareddy, J.C. Wellons, C.M. Bonfield, Epidemiology of global pediatric traumatic brain injury: qualitative review, World Neurosurg 91 (2016) 497–509.e1, https://doi.org/10.1016/j.wneu.2016.03.045.
[16] L. Gastaldi, L. Battaglia, E. Peira, D. Chirio, E. Muntoni, I. Solazzi, M. Gallarate, F. Dosio, Solid lipid nanoparticles as vehicles of drugs to the brain: current state of the art, Eur. J. Pharm. Biopharm. 87 (2014) 433–444, https://doi.org/10.1016/j.ejpb.2014.05.004.
[17] L. Schoenmaker, D. Witzigmann, J.A. Kulkarni, R. Verbeke, G. Kersten, W. Jiskoot, D.J.A. Crommelin, mRNA-lipid nanoparticle COVID-19 vaccines: structure and stability, Int. J. Pharm. 601 (2021) 120586, https://doi.org/10.1016/j.ijpharm.2021.120586.
[18] Y. Wu, A. Angelova, Recent uses of lipid nanoparticles, cell-penetrating and bioactive peptides for the development of brain-targeted nanomedicines against neurodegenerative disorders, Nanomaterials 13 (2023), https://doi.org/10.3390/nano13233004.
[19] I. Arduino, N. Depalo, F. Re, R. Dal Magro, A. Panniello, N. Margiotta, E. Fanizza, A. Lopalco, V. Laquintana, A. Cutrignelli, A.A. Lopedota, M. Franco, N. Denora, PEGylated solid lipid nanoparticles for brain delivery of lipophilic kiteplatin Pt(IV) prodrugs: an in vitro study, Int. J. Pharm. 583 (2020), https://doi.org/10.1016/j.ijpharm.2020.119351.
[20] I. Arduino, R.M. Iacobazzi, C. Riganti, A.A. Lopedota, M.G. Perrone, A. Lopalco, A. Cutrignelli, M. Cantore, V. Laquintana, M. Franco, N.A. Colabufo, G. Luurtsema, M. Contino, N. Denora, Induced expression of P-gp and BCRP transporters on brain endothelial cells using transferrin functionalized nanostructured lipid carriers: a first step of a potential strategy for the treatment of Alzheimer's disease, Int. J. Pharm. 591 (2020) 120011, https://doi.org/10.1016/j.ijpharm.2020.120011.
[21] A.C. Anselmo, Y. Gokarn, S. Mitragotri, Non-invasive delivery strategies for biologics, Nat. Rev. Drug Discov. 18 (2019) 19–40, https://doi.org/10.1038/nrd.2018.183.
[22] S.A. Wissing, O. Kayser, R.H. Müller, Solid lipid nanoparticles for parenteral drug delivery, Adv. Drug Deliv. Rev. 56 (2004) 1257–1272, https://doi.org/10.1016/j.addr.2003.12.002.
[23] Y. Liu, G. Yang, Y. Hui, S. Ranaweera, C.-X. Zhao, Microfluidic nanoparticles for drug delivery, Small 18 (2022) 2106580, https://doi.org/10.1002/smll.202106580.
[24] F. Sommonte, E. Weaver, E. Mathew, N. Denora, D.A. Lamprou, In-house innovative "diamond shaped" 3D printed microfluidic devices for lysozyme-loaded liposomes, Pharmaceutics 14 (2022) 2484, https://doi.org/10.3390/pharmaceutics14112484.
[25] I. Arduino, Z. Liu, A. Rahikkala, P. Figueiredo, A. Correia, A. Cutrignelli, N. Denora, H.A. Santos, Preparation of cetyl palmitate-based PEGylated solid lipid nanoparticles by microfluidic technique, Acta Biomater. 121 (2021) 566–578, https://doi.org/10.1016/j.actbio.2020.12.024.
[26] I. Arduino, Z. Liu, R.M. Iacobazzi, A.A. Lopedota, A. Lopalco, A. Cutrignelli, V. Laquintana, L. Porcelli, A. Azzariti, M. Franco, H.A. Santos, N. Denora, Microfluidic preparation and in vitro evaluation of iRGD-functionalized solid lipid nanoparticles for targeted delivery of paclitaxel to tumor cells, Int. J. Pharm. 610 (2021) 121246, https://doi.org/10.1016/j.ijpharm.2021.121246.
[27] R.M. Iacobazzi, I. Arduino, R. Di Fonte, A.A. Lopedota, S. Serratì, G. Racaniello, V. Bruno, V. Laquintana, B.-C. Lee, N. Silvestris, F. Leonetti, N. Denora, L. Porcelli, A. Azzariti, Microfluidic-assisted preparation of targeted pH-responsive polymeric micelles improves gemcitabine effectiveness in PDAC: in vitro insights, Cancers 14 (2022), https://doi.org/10.3390/cancers14010005.
[28] D. Fondaj, I. Arduino, A.A. Lopedota, N. Denora, R.M. Iacobazzi, Exploring the microfluidic production of biomimetic hybrid nanoparticles and their

pharmaceutical applications, Pharmaceutics 15 (2023), https://doi.org/10.3390/pharmaceutics15071953.
[29] G.M. Whitesides, The origins and the future of microfluidics, Nature 442 (2006) 368–373, https://doi.org/10.1038/nature05058.
[30] J.P. Martins, G. Torrieri, H.A. Santos, The importance of microfluidics for the preparation of nanoparticles as advanced drug delivery systems, Expet Opin. Drug Deliv. 15 (2018) 469–479, https://doi.org/10.1080/17425247.2018.1446936.
[31] E. Weaver, C. O'Hagan, D.A. Lamprou, The sustainability of emerging technologies for use in pharmaceutical manufacturing, Expet Opin. Drug Deliv. 19 (2022) 861–872, https://doi.org/10.1080/17425247.2022.2093857.
[32] F. Sommonte, I. Arduino, R.M. Iacobazzi, M. Tiboni, F. Catalano, R. Marotta, M. Di Francesco, L. Casettari, P. Decuzzi, A.A. Lopedota, N. Denora, Microfluidic assembly of "Turtle-Like" shaped solid lipid nanoparticles for lysozyme delivery, Int. J. Pharm. 631 (2023) 122479, https://doi.org/10.1016/j.ijpharm.2022.122479.
[33] S. Serratì, M. Guida, R. Di Fonte, S. De Summa, S. Strippoli, R.M. Iacobazzi, A. Quarta, I. De Risi, G. Guida, A. Paradiso, L. Porcelli, A. Azzariti, Circulating extracellular vesicles expressing PD1 and PD-L1 predict response and mediate resistance to checkpoint inhibitors immunotherapy in metastatic melanoma, Mol. Cancer 21 (2022), https://doi.org/10.1186/s12943-021-01490-9.
[34] I. Arduino, R. Di Fonte, M. Tiboni, L. Porcelli, S. Serratì, D. Fondaj, T. Rafaschieri, A. Cutrignelli, G. Guida, L. Casettari, A. Azzariti, A.A. Lopedota, N. Denora, R. M. Iacobazzi, Microfluidic development and biological evaluation of targeted therapy-loaded biomimetic nano system to improve the metastatic melanoma treatment, Int. J. Pharm. 650 (2024), https://doi.org/10.1016/j.ijpharm.2023.123697.
[35] H.T. Lam, B. Le-Vinh, T.N.Q. Phan, A. Bernkop-Schnürch, Self-emulsifying drug delivery systems and cationic surfactants: do they potentiate each other in cytotoxicity? J. Pharm. Pharmacol. 71 (2019) 156–166, https://doi.org/10.1111/jphp.13021.
[36] B. Weksler, I.A. Romero, P.O. Couraud, The hCMEC/D3 cell line as a model of the human blood brain barrier, Fluids Barriers CNS 10 (2013), https://doi.org/10.1186/2045-8118-10-16.
[37] L. Pisani, R. Farina, M. Catto, R.M. Iacobazzi, O. Nicolotti, S. Cellamare, G. F. Mangiatordi, N. Denora, R. Soto-Otero, L. Siragusa, C.D. Altomare, A. Carotti, Exploring basic tail modifications of coumarin-based dual acetylcholinesterase-monoamine oxidase B inhibitors: identification of water-soluble, brain-permeant neuroprotective multitarget agents, J. Med. Chem. 59 (2016) 6791–6806, https://doi.org/10.1021/acs.jmedchem.6b00562.
[38] A. Lopalco, A. Lopedota, F. Aurelio, F. la Forgia, S. Fontana, M. Franco, N. Denora, Stability of diazepam enema extemporaneous formulation in manzoni base, Int. J. Pharm. Compd. 25 (2021) 427–430. http://europepmc.org/abstract/MED/34623969.
[39] J. Fan, S. Li, Z. Wu, Z. Chen, Chapter 3 - diffusion and mixing in microfluidic devices, in: H.A. Santos, D. Liu, H. Zhang (Eds.), Microfluidics for Pharmaceutical Applications, William Andrew Publishing, 2019, pp. 79–100, https://doi.org/10.1016/B978-0-12-812659-2.00003-X.
[40] I.V. Zhigaltsev, N. Belliveau, I. Hafez, A.K.K. Leung, J. Huft, C. Hansen, P.R. Cullis, Bottom-up design and synthesis of limit size lipid nanoparticle systems with aqueous and triglyceride cores using millisecond microfluidic mixing, Langmuir 28 (2012) 3633–3640, https://doi.org/10.1021/la204833h.
[41] N.M. Belliveau, J. Huft, P.J. Lin, S. Chen, A.K. Leung, T.J. Leaver, A.W. Wild, J. B. Lee, R.J. Taylor, Y.K. Tam, C.L. Hansen, P.R. Cullis, Microfluidic synthesis of highly potent limit-size lipid nanoparticles for in vivo delivery of siRNA, Mol. Ther. Nucleic Acids 1 (2012) e37, https://doi.org/10.1038/mtna.2012.28.
[42] Microfluidic ChipShop, 2024. https://www.microfluidic-chipshop.com/catalogue/microfluidic-chips/polymer-chips/micro-mixer/micro-mixer-fluidic-187/. (Accessed 26 March 2024).
[43] E. Weaver, F. Sommonte, A. Hooker, N. Denora, S. Uddin, D.A. Lamprou, Microfluidic encapsulation of enzymes and steroids within solid lipid nanoparticles, Drug Deliv Transl Res 14 (2024) 266–279, https://doi.org/10.1007/s13346-023-01398-5.
[44] T. Mizui, M. Kojima, Recent advances in the biology of BDNF and the newly identified pro-peptide. https://doi.org/10.29245/2572.942X/2018/6.1228, 2018.
[45] M. Rakotoarisoa, B. Angelov, M. Drechsler, V. Nicolas, T. Bizien, Y.E. Gorshkova, Y. Deng, A. Angelova, Liquid crystalline lipid nanoparticles for combined delivery of curcumin, fish oil and BDNF: in vitro neuroprotective potential in a cellular model of tunicamycin-induced endoplasmic reticulum stress, Smart Mater Med 3 (2022) 274–288, https://doi.org/10.1016/j.smaim.2022.03.001.
[46] Y. Wu, M. Rakotoarisoa, B. Angelov, Y. Deng, A. Angelova, Self-assembled nanoscale materials for neuronal regeneration: a focus on BDNF protein and nucleic acid biotherapeutic delivery, Nanomaterials 12 (2022), https://doi.org/10.3390/nano12132267.
[47] S. Pilakka-Kanthikeel, V.S.R. Atluri, V. Sagar, S. Saxena, M. Nair, Targeted brain derived neurotropic factors (BDNF) delivery across the blood-brain barrier for neuro-protection using magnetic nano carriers: an in-vitro study, PLoS One 8 (2013), https://doi.org/10.1371/journal.pone.0062241.
[48] G. Graverini, V. Piazzini, E. Landucci, D. Pantano, P. Nardiello, F. Casamenti, D. E. Pellegrini-Giampietro, A.R. Bilia, M.C. Bergonzi, Solid lipid nanoparticles for delivery of andrographolide across the blood-brain barrier: in vitro and in vivo evaluation, Colloids Surf. B Biointerfaces 161 (2018) 302–313, https://doi.org/10.1016/j.colsurfb.2017.10.062.
[49] M.P. Soni, N. Shelkar, R. Gaikwad, G.R. Vanage, A. Samad, P.V. Devarajan, Buparvaquone loaded solid lipid nanoparticles for targeted delivery in theleriosis, J. Pharm. BioAllied Sci. 6 (2014) 22–30. https://api.semanticscholar.org/CorpusID:23454581.
[50] M.A. Schubert, C.C. Müller-Goymann, Characterisation of surface-modified solid lipid nanoparticles (SLN): influence of lecithin and nonionic emulsifier, Eur. J. Pharm. Biopharm. 61 (2005) 77–86, https://doi.org/10.1016/j.ejpb.2005.03.006.
[51] T. Ilić, J.B. Đoković, I. Nikolić, J.R. Mitrović, I. Pantelić, S.D. Savić, M.M. Savić, Parenteral lipid-based nanoparticles for CNS disorders: integrating various facets of preclinical evaluation towards more effective clinical translation, Pharmaceutics 15 (2023), https://doi.org/10.3390/pharmaceutics15020443.
[52] A. Alamri, A. Alqahtani, T. Alqahtani, A. Al Fatease, S.A. Asiri, R.M. Gahtani, S. M. Alnasser, J.M.M. Mohamed, F. Menaa, Design, physical characterizations, and biocompatibility of cationic solid lipid nanoparticles in HCT-116 and 16-HBE cells: a preliminary study, Molecules 28 (2023), https://doi.org/10.3390/molecules28041711.
[53] K.W. Wu, C. Sweeney, N. Dudhipala, P. Lakhani, N.D. Chaurasiya, B.L. Tekwani, S. Majumdar, Primaquine loaded solid lipid nanoparticles (SLN), nanostructured lipid carriers (NLC), and nanoemulsion (NE): effect of lipid matrix and surfactant on drug entrapment, in vitro release, and ex vivo hemolysis, AAPS PharmSciTech 22 (2021), https://doi.org/10.1208/s12249-021-02108-5.
[54] V.S.K. Nishihira, A.M. Rubim, M. Brondani, J.T. dos Santos, A.R. Pohl, J. F. Friedrich, J.D. de Lara, C.M. Nunes, L.R. Feksa, E. Simão, R. de Almeida Vaucher, M.G. Durruthy, L.V. Laporta, V.C. Rech, In vitro and in silico protein corona formation evaluation of curcumin and capsaicin loaded-solid lipid nanoparticles, Toxicol. Vitro 61 (2019) 104598, https://doi.org/10.1016/j.tiv.2019.104598.
[55] O.I. Schmidt, C.E. Heyde, W. Ertel, P.F. Stahel, Closed head injury—an inflammatory disease? Brain Res. Rev. 48 (2005) 388–399, https://doi.org/10.1016/j.brainresrev.2004.12.028.
[56] K. Fluiter, A.L. Opperhuizen, B.P. Morgan, F. Baas, V. Ramaglia, Inhibition of the membrane attack complex of the complement system reduces secondary neuroaxonal loss and promotes neurologic recovery after traumatic brain injury in mice, J. Immunol. 192 (2014) 2339–2348, https://doi.org/10.4049/jimmunol.1302793.
[57] Bo-Michael Bellander, Sim K. Singhrao, Marcus Ohlsson, Per Mattsson, Mikael Svensson, Complement activation in the human brain after traumatic head injury, J. Neurotrauma 18 (2004) 1295–1311.
[58] D.G. Hernandez-Ontiveros, N. Tajiri, S. Acosta, B. Giunta, J. Tan, C.V. Borlongan, Microglia activation as a biomarker for traumatic brain injury, Front. Neurol. 4 (MAR) (2013), https://doi.org/10.3389/fneur.2013.00030.
[59] D. Tewari, A.N. Sah, S. Bawari, S.F. Nabavi, A.R. Dehpour, S. Shirooie, N. Braidy, B. L. Fiebich, R.A. Vacca, S.M. Nabavi, Role of nitric oxide in neurodegeneration: function, regulation, and inhibition, Curr. Neuropharmacol. 19 (2020) 114–126, https://doi.org/10.2174/1570159x18666200429001549.
[60] M. Pulido-Salgado, J.M. Vidal-Taboada, G.G.D. Barriga, C. Solà, J. Saura, RNA-Seq transcriptomic profiling of primary murine microglia treated with LPS or LPS + IFNγ, Sci. Rep. 8 (2018) https://doi.org/10.1038/s41598-018-34412-9.